SMT-LEARNER: MOVEMENT TRAJECTORY LEARNING TO DECODE MOTOR CONTROL STRATEGIES

Anonymous authors
Paper under double-blind review

ABSTRACT

Spatiotemporal movement trajectory (SMT) representation is essential to understanding the motor skill learning and adaptation strategies that inform neurorehabilitation practices. Movement performance metrics (i.e., speed, accuracy) are insufficient to characterize motor control strategies and learning patterns, particularly in individuals with disordered movement. Motor skill learning patterns require an interpretable sequential SMT representation that preserves spatial, temporal, and performance variables. We present a novel SMT-Learner with transformer autoencoders that optimize performance-aware contrastive and adaptive transfer losses, combining cross-task and cross-subject transfer paradigms. SMT-Learner encodes trajectories into a high-dimensional latent space and enables motor performance-aware learning. We introduce an Exploration-Exploitation (E-E) analytical framework that quantifies motor skill learning and control strategies to balance different movement patterns and micro-adaptation. We tested and validated the SMT-Learner with two visuomotor reaching datasets: (1) a prospectively obtained cohort of term and preterm children's motor learning and performance of unimanual and bimanual tasks, and (2) extensively overtrained non-human primates performing target-directed reaching movements. Our ablation and baseline comparison across geometric, statistical, and clustering metrics demonstrated that SMT-Learner outperformed with the lowest reconstruction error (0.086) and optimized clinical correlation with motor performance variables. Investigated E-E patterns significantly correlated with the early and late stages of motor learning and speed-accuracy trade-offs principles. The SMT-Learner framework provides an efficient computational approach to quantify motor learning strategies; potential advanced downstream applications in developmental assessment, neurorehabilitation monitoring, and movement optimization in robotics or brain-computer interfacing.

1 INTRODUCTION

Recent research in developing analytic tools for motion and kinematic data has applied ML/AI methods to understand motor recovery patterns and prognosis in individuals undergoing neurorehabilitation (i.e., children with cerebral palsy Rapuc et al. (2024), traumatic brain injury Uparela-Reyes et al. (2024); Balaji et al. (2023), post stroke survivors Campagnini et al. (2022)) Choo & Chang (2022); Butepage et al. (2017); Song et al. (2017); Reinkensmeyer et al. (2016). Spatiotemporal movement analysis has created new opportunities to study human motor behavior Wulff et al. (2019); Renso et al. (2013), specifically in movement patterns Viviani & Terzuolo (1982); Kalayeh et al. (2015); Wulff et al. (2019); Long & Nelson (2013), motor rehabilitation Kitago & Krakauer (2013); Levin et al. (2010); van Andel et al. (2008); Murphy et al. (2011), and its underlying neural correlates Svoboda & Li (2018); Gallego et al. (2018). For example, ML-based kinematic analysis using spatial van Andel et al. (2008) or temporal Murphy et al. (2011) parameters of upper extremity tasks can predict movement smoothness and track movement quality. How different motor control strategies are related to upper extremity performance over long-term practice of a motor rehabilitation task is still challenging to decode. Understanding the motor behavior and learning processes from high-repetition and high-density spatiotemporal movement data necessitates new representation learning to decode the patterns. Research in motor learning and development involving spatiotemporal movement trajectories (SMT) utilizes diverse data capture and measurement technologies, including marker and markerless 3D motion capture systems Menolotto et al. (2020), wearable inertial

measurement units (IMUs) Zhou & Hu (2008), that provide high spatial-temporal resolution for precise movement tracking. Digital tablets (e.g., iPads) have recently emerged as powerful tools to capture spatiotemporal aspects of movement, particularly in handwriting, individual finger movement, bimanual coordination, and fine motor skills Palmis et al. (2019); Mia et al. (2024). Importantly, these devices can capture high-resolution temporal and spatial data, including position coordinates, time, velocity, and acceleration during movement execution, needed for motor learning analyses. There are several ML/DL models extensively applied to spatiotemporal trajectory and motion analysis, such as motor recovery prediction Campagnini et al. (2022); Vu et al. (2018) or gait recovery Prakash et al. (2018); Hor et al. (2023), robotics Finn et al. (2016); Saveriano et al. (2023), pedestrian movement analysis Alahi et al. (2016); Rudenko et al. (2020), and autonomous vehicles Schwarting et al. (2018); Maqueda et al. (2018); Kuutti et al. (2020). However, SMT analysis in motor learning studies requires different approaches to decode motor control strategies, micro-adaptation, and learning progress, which potentially impact clinical intervention.

In our recent investigation on motor skill learning and performance using an iPad-based gamified visuomotor task among term and preterm school-aged children (N=72, Ages 5-8 years), a new computational problem was identified while interpreting control strategies, due to the nature of non-linear movement dynamics. Compared to term-born children, preterm children have a significantly higher risk of motor delays, which affects their ability to learn and perform motor skills compared to term-born peers Foulder-Hughes & Cooke (2003); Uusitalo et al. (2020); Patel (2016); Allotey et al. (2018); Carter & Msall (2018); Spittle et al. (2016). In addition to lower motor performance, preterm children's ability to learn new motor skills may be impacted due to maladaptive developmental patterns Ortinau & Neil (2015) and differences in brain structures important for sensorimotor function Liu et al. (2010); Adams et al. (2010); Shimony et al. (2016). However, the underlying motor learning strategies used by preterm and term children are difficult to interpret from conventional motor performance parameters. Indeed, there is a distinction in movement variation and adaptation between these two groups. Figure 1 exemplifies an individual's motor learning, where low (during practice) and high (retention) cumulative success rates, the probability of reaching the target at least once over a series of independent trials, had nearly similar movement path lengths. Therefore, a research gap exists in understanding motor learning progress and control strategies from movement data and performance variables.

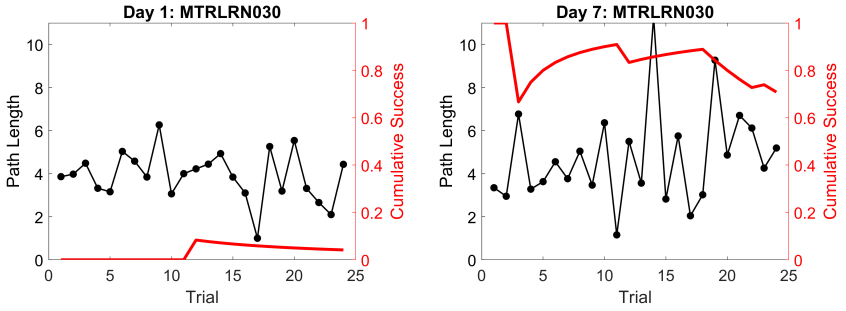

(a) Participant 030 had a very low success rate (red curve) relative to a moderate level of accuracy (4 times ideal path length)

(b) After training, success rate increased to greater than 70% but the accuracy remained at a similar (and perhaps greater) level

Figure 1: Example of a participant's motor skills learning from Day 1 to Day 7, while a traditional parameter (i.e., movement path length) could not capture learning or overall performance on a task. In this task, participants moved a joystick up and down to map movement on a 2D game scene to achieve a target-directed destination from a source.

Existing DL-based trajectory autoencoder and embedding methods, such as STTraj2Vec Zhu et al. (2024), Variational Auto-Encoders (VAEs) Ivanovic et al. (2020), Sequence-to-Sequence Auto-Encoders Sarkar & Ghose (2018); Wang et al. (2022), while effective in movement prediction and classification yet challenging to interpret complex non-linear relationships in movement patterns. Transformer architectures with self-attention mechanisms Shaw et al. (2018) and self-supervised pre-training approaches (i.e., TimeContrast Guo et al. (2022), MovementContrast Shah et al. (2023)) are capable of capturing sequence dependencies and temporal relationships. However, the repetitive task-based motor training and therapy in rehabilitation practices require more sophisticated methods, which will

preserve trial-to-trial performance variables along with temporal and spatial patterns. This problem motivated the design of a new SMT representation learning framework.

We propose a novel SMT-Learner that combines joint learning with movement performance-aware multi-contrastive loss and adaptive transfer learning. A new human SMT dataset (D_1) was created from prior motor skill learning and performance investigation to train and evaluate the model. To cross-validate the generalized applicability of SMT-Learner, evaluate with another hand reaching trajectory dataset (D_2) of highly trained non-human primates Scott et al. (2001); Scott & Kalaska (1997). Moreover, we introduce an exploration-exploitation (E-E) analytical framework to quantify motor control strategies and micro-adaptation from the representation, categorized as i) exploratory strategy Svoboda & Li (2018) – where current movement does not correlate with previous movement attempts, and ii) exploitative strategy Gallego et al. (2018) – where prior movements predict current movement. We assessed how movement exploration and exploitation differed between: a) two types of hand movements (unimanual and bimanual), b) term and preterm children, and c) early and late motor learning phases. To provide further SMT-Learner interpretability, we conducted a case study analysis showing two distinct optimal strategies captured by the framework: (1) Curvature optimization to near-straight paths, and (2) Stepwise rectilinear movements with right-angle directional changes.

Neuroscientific Foundation of E-E Framework: Exploitation/exploration are well-established concepts to study human and other species' cognitive and motor learning evaluation. E-E frameworks Wyatt et al. (2024) found useful for studying how humans make decisions with known outcomes versus acquiring new information and new outcomes with less certainty. For example, children tend to use more explorative strategies early in development to gather more information, even when this approach may be less rewarded Blanco & Sloutsky (2024). Human visual exploration studies demonstrated Bayesian optimal foraging models Cain et al. (2012) and uncertainty reduction mechanisms Mirza et al. (2018) that are parallel to movement exploration/exploitation. Established principles of motor learning through adaptive combination of motor primitives Thoroughman & Shadmehr (2000) and complementary roles of neural circuits Doya (2000) support E-E mechanisms in biological motor systems. In non-human motor learning studies, E-E concepts are significantly applied to understand motor learning behaviours and neural dynamics. One rodent exploratory behavior study Mumby et al. (2002) demonstrated corticostriatal dynamics that reinforce the reduction of movement variability in repetitive motor skill learning Dhawale et al. (2017) and refinement of muscle synergies Santos et al. (2015), supporting distinction in early exploration and late exploitation strategies. Moreover, this principle also explained how young songbirds produce highly variable vocalizations and strategically transition to stereotyped songs with vocal motor learning Ölveczky et al. (2005); Kojima et al. (2018).

We statistically validated the following hypotheses to demonstrate our framework's effectiveness and its clinical implications. **Hypothesis 1a:** *Early learning will be more explorative and will shift to an exploitative strategy in the late learning phase in all participants.* **Hypothesis 1b:** *Preterm children will exhibit a higher exploration/exploitation (E-E) ratio than term children, particularly for the bimanual skill learning task.* Our cross-validation hypotheses are: **Hypothesis 2a:** *As monkeys were extensively overtrained (D_2), their overall E-E ratio will be significantly lower than that of a human learner on an untrained task.* **Hypothesis 2b:** *The E-E ratio will decrease over sequential trials of the same motor learning task, even in well-trained non-human primates, reflecting a micro-adaptation learning process.* The methodological validation will also confirm a speed-accuracy trade-off principle of motor skill development Plamondon & Alimi (1997); Spieser et al. (2017); Molina et al. (2019) preserved by SMT-Learner representation. **Hypothesis 3a:** *Movement performance variables such as movement speed or accuracy will correlate negatively or positively, respectively, with E-E ratio.* This hypothesis will clinically validate our framework's relationship to conventional motor performance variables. Finally, we discuss the potential of the presented approach for clinical translation with limitations and future directions.

2 PRELIMINARY

Movement path. A real movement path P is a continuous function of time mapping 2D spatial coordinates. Movement path is a function defined as, $P : [0, T] \rightarrow \mathbb{R}^d$, where T is the total time duration of a movement path and for each time point $t \in [0, T]$, $P(t) = (x_t, y_t)$, return a 2D position with x-coordinate and y-coordinate value in the movement space.

Trajectory. A trajectory ($\mathcal{T}$) of a moving object is a sequence of positions over time in the movement space, define as $\mathcal{T} = \{(x_1, y_1, t_1), (x_2, y_2, t_2), \ldots (x_n, y_n, t_n)\}$. Where (x_i, y_i) represents spatial coordinates at time t_i with $0 = t_1 < t_2 < \ldots t_n = T$ and n is the number of recorded positions.

Problem Formulation. Given a dataset of N spatiotemporal movement trajectories, D $= \{ \mathcal{T}_1, \mathcal{T}_2, \ldots, \mathcal{T}_N \}$, where each trajectory $\mathcal{T}_i$ defined as $\mathcal{T}_i = \{(x_j, y_j, t_j) | \, j = 1, 2, \ldots m\}$. Each trajectory has associated temporal metadata $M_i = \{m_1, m_2, \ldots, m_k\} \subseteq \{pid, task, c\_time, rmsd, is\_success\}$. Here, c_time is the total completion time of the movement from source to destination in seconds, $task$ indicates experimental visuomotor/movement task, $rmsd$ is root mean square deviation of the original movement path from direct straight line ($source \rightarrow destination$), and $is\_success$ is a flag (0 or 1) that indicate the successfully reaching the destination. We aim to train a trajectory autoencoder to learn a mapping function $f_\theta : \mathcal{T} \rightarrow \mathbb{R}^d$ that transforms each variable-length trajectory into a d-dimensional vector, $\varepsilon_i = f_\theta(\mathcal{T}_i) \in \mathbb{R}^d$ and captures spatio-temporal patterns with preservation of movement performance metrics. We focus on developing SMT-Learner, combining a self-attention encoder and self-supervised pre-training to optimize trajectory reconstruction and movement performance-aware multi-contrastive loss, enabling transfer learning. The goal is to achieve embedding $\mathbb{R}^d$ as a representation of SMT to conduct downstream experiments, specifically the motor learning behavior and the detection of control strategies using E-E analysis.

3 METHODOLOGY

SMT-Learner builds upon transformer-based sequential processing Vaswani et al. (2017) and self-supervised contrastive learning Chen et al. (2020), which includes movement performance meta-criterions as contrastive loss for representing trajectories into the embedded space and enables transfer learning Zhang & Gao (2022). SMT-Learner is driven by motor learning principles, designed to learn domain-agnostic representations of planar reaching tasks to decode motor learning and control strategies—measured through speed, accuracy, and success.

3.1 TRAJECTORY PROCESSING

Normalization. A normalized trajectory $\mathcal{T}^{'}$ is a standardized representation of spatial curve that resolves the variable-lengths and geometric constraints of randomize start and target of a moving object. A trajectory transformation process $\mathcal{N}$ applied to normalize a trajectory, $\mathcal{T}^{'} = \mathcal{N}(\mathcal{T}) = \{(P_j, t_j) | \, j = 1, 2, 3 \ldots, m\}$, where $\mathcal{T}^{'}$ origin-centered at $\mathcal{T}_1^{'} = (P_{(0,0)}, t_1)$, target-aligned at $\mathcal{T}_m^{'} = (P_{(0,0)}, t_m)$. transformation process $\mathcal{N}$ involves:

(i) Translate position P of the trajectory to center: $P_i^{'} = P_i - P_1 = \{x_i - x_1, y_i - y_1\}$,

(ii) Rotation by θ angles to align with target position: $R(\theta) = \begin{vmatrix} x_i \cos\theta - y_i \sin\theta \\ x_i \sin\theta + y_i \cos\theta \end{vmatrix}$, and

(iii) Trajectory is scaled by factor s to finalize position into a specific magnitude: $s = \frac{\left\| \overrightarrow{V}_{target} \right\|}{\left\| \overrightarrow{V}_{end} \right\|}$,

where $\overrightarrow{V}_{target} = P_{(0,1)} - P_{(0,0)}$ and $\overrightarrow{V}_{end} = P_n - P_1$. Finally, positional normalization of trajectory is transformed by $\mathcal{T}_{norm} = P_i^{'} \mathrm{x}\, R(\theta) \mathrm{x}\, s$.

The rotating/scaling trajectories to a canonical frame removes absolute direction and can obscure biomechanical/cognitive asymmetries. We kept this normalization to simplify trajectory learning while preserving spatial and temporal structure, but we have incorporated directional semantics by adding the target direction angle, $\theta_i = atan2(P_n - P_i)$ to each timestep input and optionally the rotation angle used in normalization as auxiliary inputs.

Resampling. For each normalized trajectory sequence with a given length *n*, we applied a parameterized approach to get fixed *m* points that preserve spatial and temporal characteristics. A uniform space parameter, $u_j^{'} = \frac{j-1}{m-1}, for j = 1, 2, 3, \ldots, m$ is defined to obtain exactly m resampled points by identifying segments in the original trajectory where $u_i \leq u_j^{'} < u_{i+1}$, where $u_i = \frac{i-1}{n-1}$, for

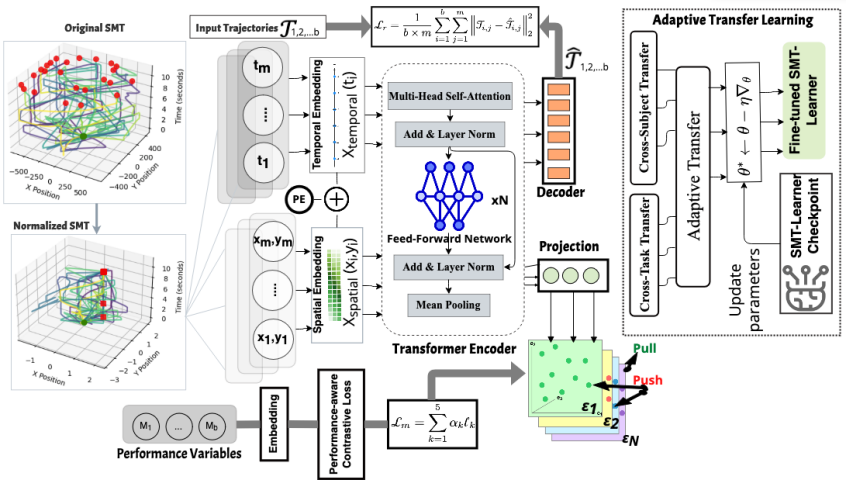

Figure 2: Architecture of SMT-Learner with transfer paradigm

$i = 1, 2, 3, \ldots, n$. An interpolation weight, $\alpha_j = \frac{u_j^{'} - u_i}{u_i + 1 - u_i}$ is used to calculate each dimension of the trajectory using the following equations: $x_j^{'} = (1 - \alpha_j)\, x_i + \alpha_j x_{i+1}$, $y_j^{'} = (1 - \alpha_j)\, y_i + \alpha_j y$, and $t_j^{'} = (1 - \alpha_j)\, t_i + \alpha_j t_{i+1}$.

3.2 SMT-Learner and Adaptive Transfer

The SMT-Learner consists of five layers (Figure 2): i) dual-stream spatial and temporal embedding, ii) transformer encoder with multi-head self-attention and feed-forward network, iii) dual-headed output with projection and decoder, iv) a movement performance-aware contrastive learning with transfer paradigm, and v) a joint optimization with contrastive and reconstruction loss. The spatial (x_i, y_i) and temporal (t_i) components of each point in the normalized trajectory $\mathcal{T}$ are projected into a D-dimensional space using $X_{spatial}$ and $X_{temporal}$ linear transformer with a positional encoder. Spatial & temporal embedding results a tensor X of shape $(b \times m \times D)$, where b is the batch size and m is the number of points in a trajectory, which is the input of the Transformer encoder. Two parallel branches processed the output of the transformer encoder to generate the final embedded representation and reconstructed trajectory using a Projection Head and Decoder, respectively. Embedded output of the non-linear Projection Head He et al. (2020) is $E = ReLU\left(w_1^{proj}.Z_{global} + b_1^{proj}\right) w_2^{proj} + b_2^{proj}$, with shape $(b \times d)$ contains $E \subset (\varepsilon_1, \varepsilon_2, ..\varepsilon_b)$ embeddings where each $\varepsilon_i \in \mathbb{R}^d$. Embeddings ε_i was used for constative loss calculation. The Decoder reconstructed the original trajectory as $\hat{\mathcal{T}} = Reshape\left(w^{dec}.Z_{global} + b^{dec}\right)$. The reconstructed trajectory used to calculate the reconstruction loss $(\mathcal{L}_r)$ using Equation 1.

$$\mathcal{L}_r = \frac{1}{b \times m} \sum_{i=1}^{b} \sum_{j=1}^{m} \left\| \mathcal{T}_{i,j} - \hat{\mathcal{T}}_{i,j} \right\|_2^2 \tag{1}$$

3.2.1 Performance-aware Contrastive Learning

The model learns the representation in embedded space $\varepsilon \in \mathbb{R}^d$ from the motor performance meta criterion (M_i) using "pull" and "push" operations, where pull similar trajectories or push dissimilar ones based on the multi-contrastive loss function $(\mathcal{L}_m)$ as calculated using Equation 2 and 3.

$$\mathcal{L}_m = \sum_{k=1}^{5} \alpha_k \ell_k \tag{2}$$

$$\ell_k = \frac{\sum_i \sum_{j \neq i} \psi_k\,(i,j) \log \frac{e^{\varepsilon_i \cdot \varepsilon_j / \tau}}{\sum_{l \neq i} e^{\varepsilon_i \cdot \varepsilon_l / \tau}}}{\sum_i \sum_{j \neq i} \psi_k(i,j) + \complement} \tag{3}$$

Where ℓ_k is loss components for corresponding meta criterion m_k and weight factor α_k as $\sum_{k=1}^{k} \alpha_k = 1$. $\complement = e^{-6}$ to avoid numerical instability. For each batch of embedded trajectories, E, contrastive loss components ℓ_k are computed based on the similarity matrix (ψ_k) for meta criterion k with a temperature parameter τ Wang & Isola (2020). Trajectory meta criterion completion time (*c_time*), root mean square deviation (*rmsd*) and successfully reaching the destination ($success$) have been used as specialized similarity measures. Let's define the rmsd distance as d, while the similarity between two trajectories ε_i and ε_j from batch E is computed by Equation 4.

$$\psi_{rmsd}(i,j) = 1 - \frac{|d_i - d_j|}{\max_{k,l} |d_k - d_l| + \complement} \tag{4}$$

Here, $\max_{k,l} |d_k - d_l|$ find the max difference in sequential paired samples of E. Completion time contrastive loss captured comparable timeframe patterns to pull or push embeddings based on the similarity calculation. Other two similarity matrices, $\psi_{c\_time}(i,j)$ and $\psi_{success}(i,j)$ capture movement speed and efficiency to learn representation. Finally, the participant ID (pid) and movement tasks ($task$) information were used as cross-subject and cross-task knowledge transfer to balance learning with specific and generalized patterns.

3.2.2 Adaptive Learning with Cross-Task and Cross-Subject Transfer

The characteristics of movement trajectory in rehabilitation or robotics space depend on the task executed, which impacts the trajectory shape, such as opening a door or moving an object from source to destination using only up-down, left-right actions. Cross-task knowledge transfer is important to preserve task-specific information and movement patterns in the representation space Shi et al. (2023). Whereas, the cross-subject transfer paradigm allows flexible control on subject-specific knowledge learned across all other subjects, for a target subject to generalize the learning in offline mode. Our transfer process simultaneously optimized joint losses $\mathcal{L}_{total} = \mathcal{L}_r + \mathcal{L}_m$. For a transfer paradigm (i.e., cross-task, cross-subject), two hyperparameters (λ_1 and λ_2) with a transfer-specific regularization are applied to optimize loss and appropriate separation between different subjects and tasks. Equations 5 and 6 update weights for a specific transfer type, where $\text{sim}(\varepsilon_i, \varepsilon_j) = \frac{\varepsilon_i \cdot \varepsilon_j}{\|\varepsilon_i\| \|\varepsilon_j\|}$ represents cosine similarity between embeddings and $\mathbb{I}[\text{factor}_i \neq \text{factor}_j]$ is an indicator function for different tasks or subjects, respectively.

$$\mathcal{L}_{\text{transfer}} = \mathcal{L}_r + \lambda_1 \mathcal{L}_m + \lambda_2 \mathcal{L}_{\text{regularization}} \tag{5}$$

$$\mathcal{L}_{\text{regularization}} = \frac{1}{N} \sum_{i=1}^{N} \sum_{j \neq i} \max(0, \text{margin} - \text{sim}(\varepsilon_i, \varepsilon_j)) \cdot \mathbb{I}[\text{factor}_i \neq \text{factor}_j] \tag{6}$$

However, motor learning is intrinsically individualized and context-dependent Shmuelof et al. (2012). Inter-subject variability and task-specific complexity require different control strategies. Static weight transfer may reduce individual differences Long et al. (2015); Kendall et al. (2018), necessitating dynamic weight updates to capture motor signatures and knowledge transfer between participants and tasks. We combined both paradigms with an adaptive transfer mechanism Cao et al. (2010), which updates model parameters $\theta^* \leftarrow \theta - \eta \nabla_\theta$ using Equation 7.

$$\mathcal{L}^{(t)}_{\text{adaptive}}(\theta) = \mathcal{L}_r + \lambda_1 \cdot \sum_{k=1}^{5} \hat{\alpha}_k^{(t)} \cdot \mathcal{L}_k(\theta) + \lambda_2 \cdot \mathcal{L}_{\text{regularization}} \tag{7}$$

Performance-aware multi-contrastive loss components, $\sum_{k=1}^{5} \hat{\alpha}_k^{(t)} \cdot \mathcal{L}_k(\theta)$ represent the core adaptive weighting mechanism dynamically balanced transfer context. During training, time-dependent weights $\hat{\alpha}_k^{(t)}$ adjust based on improvement rates from loss history windows. Transfer-specific modulation factors emphasize different components based on whether knowledge is transferred across subjects or tasks.

3.3 Exploration-Exploitation Analytical Framework

We introduced a quantitative method, the Exploration-Exploitation (E-E) framework, to analyze the decoded learning patterns and control strategies from the SMT-Learner representation. In the motor

Table 1: Summary of SMT-Learner pretraining/finetuning results, all experiments conducted on D_1

Paradigm	Pretrain	Evaluate (target)	Zero-shot mean [95% CI]	Fine-tuned mean [95% CI]	Δ%
Exp1	D1	D1 test	1.55 [1.525, 1.575]	1.00 [0.98, 1.02]	−35.5%
Exp2	D1 Unimanual	D1 Bimanual	1.10 [1.08, 1.12]	0.55 [0.541, 0.559]	−50.0%
Exp3	D1 Term	D1 Preterm	1.05 [1.041, 1.059]	0.45 [0.441, 0.459]	−57.1%
Exp4	D1 Unimanual + Term	D1 Bimanual + Preterm	1.05 [1.041, 1.059]	0.12 [0.111, 0.129]	−88.6%

skill learning process, participants learn mastery of a task by repetition. Exploration scores measure movement diversity, and exploitation scores measure how prior movement predicts current movement. $\text{Exploration}(\varepsilon_i) = \min_{j<i} \text{Dist}(\varepsilon_i, \varepsilon_j) \times (\beta_1 + \beta_2 e^{-i\alpha})$, where, α is decay factor for trial sequence and β_1, β_2 are weights for movement novelty and trial sequence. The exploitation score measures how prior movement is predicting current movement using a window size (W_i) and a similarity matrix, $\text{Exploitation}(\varepsilon_i) = \frac{1}{|W_i|} \sum_{j \in W_i} \text{Sim}(\varepsilon_i, \varepsilon_j)$. Finally, E-E Ratio $= \frac{\text{Exploration}(\varepsilon_i)}{\text{Exploitation}(\varepsilon_i)}$, consider as a factor of sequential motor learning. We applied MIN distance (minimum Euclidean distance in embedding to any prior trial within a decayed window) and KNN algorithm with $W = 120$, $\alpha = 0.05$, $\beta_1 = 0.10$, and $\beta_2 = 0.90$, validated via average distance and density-based novelty. Three consistent patterns supported the selection of the optimized hyperparameters to compute E–E metrics. Sensitivity and clustering analyses are detailed in Appendix A.3.

4 Results & Discussion

SMT-Learner optimized all loss components in the pretraining stage to learn generalizability from the domain data (Appendix Section A.1 DATASETS). In the transfer stage, the SMT-Learner pre-trained model was fine-tuned using D_1 to update parameters based on the transfer paradigms (cross-task, cross-subject, and adaptive transfer). The complete experimental setup and transfer experiments are detailed in Appendix Section A.2 EXPERIMENTAL SETUP. We computed 5 seeds with mean ±95% confidence intervals (t-based, df=4) for all SMT-Learner transfer experiments (Exp1-Exp4), reported transfer loss ($\mathcal{L}_{\text{transfer}}$) in Table 1. Adaptive transfer loss ($\mathcal{L}^{(t)}_{\text{adaptive}}(\theta)$ with multi-temporal components dropped significantly (overall 25.4% performance improvement) compare to the SMT-Learner baseline model (Figure 3). Held-out evaluations were performed on D_2 tasks/sessions never seen during training to confirm cross-dataset generalization. $D_1 \rightarrow D_2$ zero-shot overall loss dropped 1.55 to 1.24 and 1.28 on a single task held-out samples (D_2 Experimental Task 1). Using the D_1 Preterm finetuned checkpoint (no D_2 pretraining/finetuning), the loss dropped to ∼1.18. Finally, adaptive transfer fine-tune loss reaches 0.98, evidence that SMT-Learner captures transferable motor structure rather than dataset-specific regularities and provides a scale-stable E–E metric (Appendix A.5).

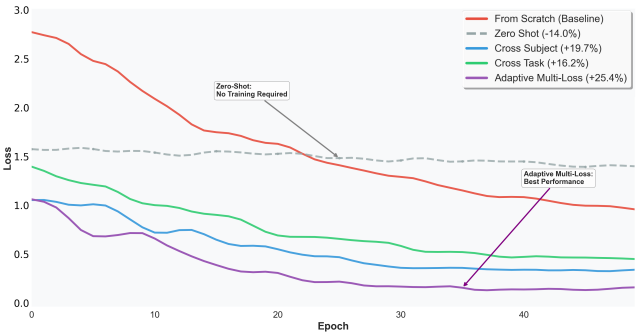

Figure 3: Comparison of adaptive transfer learning with the SMT-Learner baseline and other paradigms

4.1 Statistical Testing & Hypothesis Validation

We tested Hypotheses 1a/1b on D_1 using a three-way ANOVA (cohort, phase, task) with E–E ratio as the dependent variable. Early→late learning showed a robust shift from exploration to exploitation ($F=343.1$, $p<0.001$, $\eta^2=0.050$), with E–E decreasing from 0.667±0.056 to 0.163±0.020 (Fig. 4a, 4b). Preterm children exhibited higher E–E than term (0.444±0.059 vs. 0.386±0.030; Cohort: $F=3.72$, $p=0.054$), partially supporting 1b. Task effects were significant: bimanual > unimanual in both term (0.286±0.022 vs. 0.255±0.019; $p=0.033$) and overall (0.469±0.049 vs. 0.361±0.040; $F=10.43$,

p=0.001), consistent with delayed bimanual coordination in preterm Cooke & Foulder-Hughes (2003); Schneider et al. (2008).

For Hypotheses 2a/2b, we compared human D_1 E-E ratio to overtrained monkey D_2 reach trajectories: human E–E 0.2823±0.0128 vs. monkey 0.0542±0.0046 (t=39,957, p<10^{-4}, d=0.354), strongly supporting 2a (Fig. 4c). Block-wise slopes (120 trials; bootstrap N=5000) yielded near-linear refinement with $R^2 = 1.00$ in both species and distinct learning rates: human -0.17 [-0.19, -0.15] vs. monkey -0.008 [-0.017, -0.001], confirming 2b (Fig. 4d). These results align with literature on motor variability and expertise Spieser et al. (2017) and are summarized in Table 2.

Speed-accuracy trade-offs, widely accepted mathematical concepts in target-directed human movement, are described as neuromuscular synergy during motor execution Plamondon & Alimi (1997); Smyrnis et al. (2000); Spieser et al. (2017). Speed-accuracy trade-offs and statistical correlation between E-E ratio and performance variables (movement speed and accuracy) are illustrated in Figure 4e, 4f, and 4g. We found negative correlations between speed and accuracy in both term (r=-0.40, p<0.0001) and preterm (r=-0.36, p<0.0001) groups. We also found the E-E ratio positively correlated (Term, r=0.5 and Preterm, r=0.45) with the movement speed and negatively correlated (Term, r=-

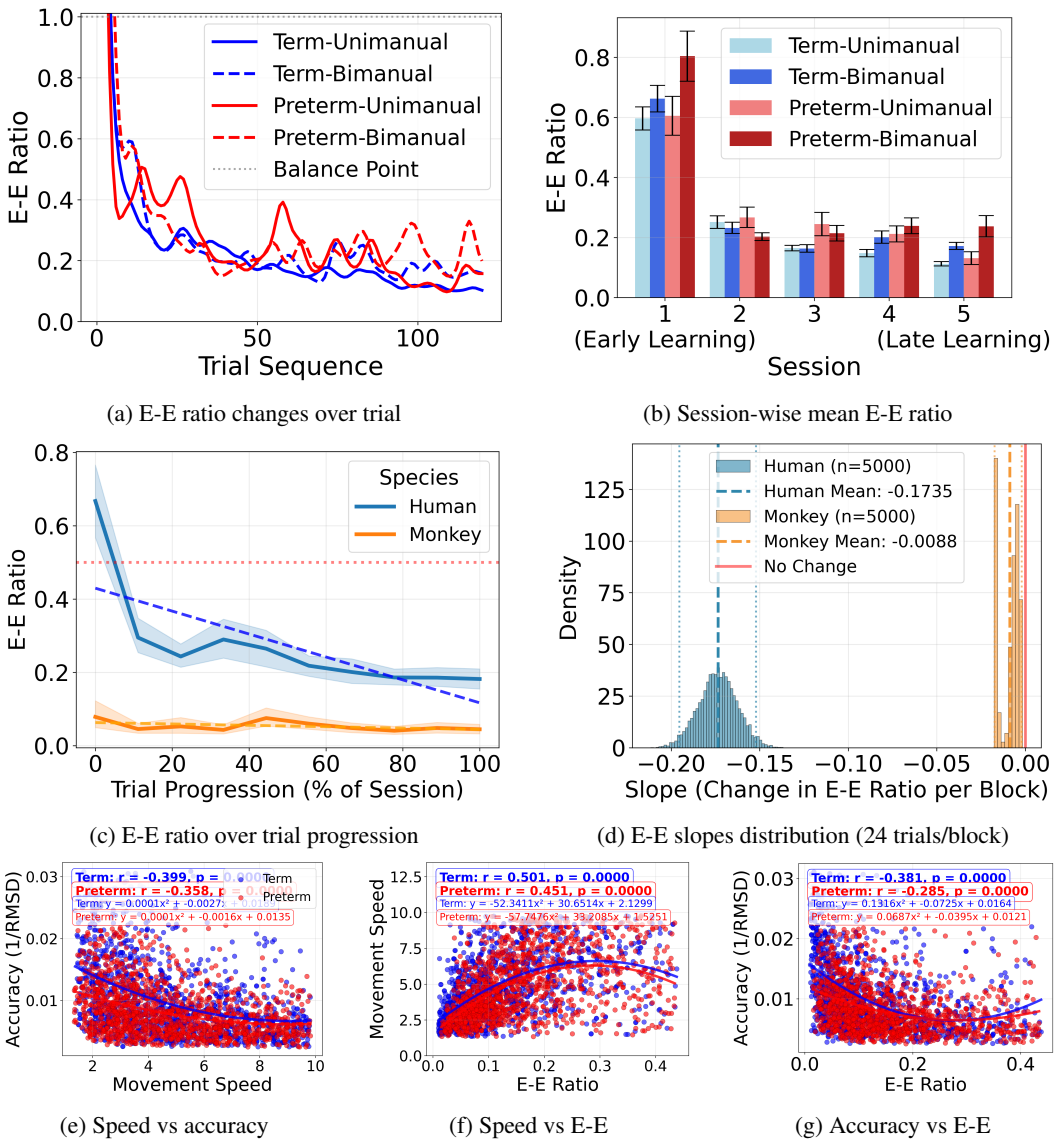

(a) E-E ratio changes over trial

(b) Session-wise mean E-E ratio

(c) E-E ratio over trial progression

(d) E-E slopes distribution (24 trials/block)

(e) Speed vs accuracy

(f) Speed vs E-E

(g) Accuracy vs E-E

Figure 4: Statistical analysis of E-E ratio in different cases: (a-b) E-E ratio changes over trial and session progression, (c-d) E-E dynamics between human learners and monkey, and (e-g) Speed-accuracy trade-offs and correlation between speed/accuracy and E-E ratio

Table 2: Evidence-based cross-matches of SMT-Learner's E–E findings with prior literature

Hyp.	Prior findings	E–E result (mean ± 95% CI)	Effect size	Test (t/p)	Interpretation
1a	Early→late stabilization in motor learning Smyrnis et al. (2000)	$0.667 \pm 0.056 \rightarrow 0.163 \pm 0.020$	$d = 0.35$	$t = 39{,}957$; $p < 10^{-4}$	E–E declines with practice; stabilization phase reached.
1b	Term vs preterm adaptability differs Hadders-Algra (2010); Dusing & Harbourne (2010) Ferrari et al. (2012)	Term: 0.386 ± 0.030; Preterm: 0.444 ± 0.059	$d = 0.28$	$p < 0.01$	Typical children show lower E–E (more exploitation).
2a	Practice reduces variability (human vs non-human) Mandelblat-Cerf et al. (2009); Dhawale et al. (2017)	Human: 0.2823 ± 0.0128; Monkey: 0.0542 ± 0.0046	$d = 0.35$	$p < 10^{-4}$	Both species exhibit reduced variability with training.
2b	Skill refinement continues post stabilization Smits-Engelsman et al. (2020); Churchland et al. (2006)	Slope: -0.17 ($R^2 = 1.0$); Monkey: -0.008 ($R^2 = 1.0$)	—	$p < 0.05$	Slow shift toward exploitation; continued refinement.

Table 3: Performance of SMT-Learner: Ablation study with contrastive and transfer configurations

Configuration	Performance Metrics								
	rMSE ↓	Ep-Err ↓	Curve-Err ↓	T-Corr ↑	R-Corr ↑	S-Corr ↑	Traj-C ↑	Task-C ↑	Sub-C ↑
Adaptive Transfer	**0.086**	**0.072**	**1.577**	**0.893**	**0.539**	**0.970**	**0.720**	**0.550**	**0.038**
No Transfer	0.145	0.089	1.634	0.756	0.423	0.912	0.685	0.487	0.025
Cross-Task Only	0.098	0.078	1.592	0.834	0.501	0.945	0.702	0.523	0.031
Cross-Subject Only	0.102	0.081	1.588	0.817	0.487	0.938	0.695	0.541	0.034
No Contrastive	0.197	0.022	1.891	0.123	0.001	-0.020	0.412	0.298	0.018
ψ_{c_time} only	0.086	0.093	1.568	0.479	0.289	0.191	0.713	0.548	0.037
ψ_{rmsd} only	0.098	0.137	1.646	-0.005	0.002	0.111	0.720	0.550	0.037
$\psi_{success}$ only	0.087	0.127	1.691	0.191	0.111	**0.993**	0.720	0.548	0.038
$+\theta$ (target direction)	0.151	0.019	1.787	**0.980**	0.539	0.910	0.720	0.548	0.038
$+\theta$+rotation angle	0.111	0.015	1.903	0.929	**0.652**	0.940	0.720	0.548	0.038

0.38 and Preterm, r=-0.29) with the movement accuracy. These findings validate our framework's relationship to the clinical assessment of motor performance and captured speed-accuracy trade-offs.

A case study is presented in Appendix Section A.4, where we demonstrate the E-E matric capable of detecting two optimal control strategies (Curvature and Stepwise).

4.2 SMT-Learner Performance Evaluation

We applied geometric, statistical, and clustering neighborhood analysis to evaluate the quality and characteristics of SMT-Learner representation. Assessment metrics are as follows: (i) Trajectory reconstruction quality: Reconstruction Mean Squared Error (rMSE), Mean Endpoint Error (Ep-Err), and Mean Curvature Error (Curve-Err); (ii) *Statistical correlation with movement performance variables:* Completion time (considered as movement speed) correlation (T-Corr), correlation with the root mean square deviation of movement (considered as accuracy) from the optimal path (R-Corr), and correlation with successfully reaching the target (S-Corr); and (iii) *Clustering neighborhood consistency:* trajectory shape consistency (Traj-C), cross-task consistency (Task-C), and cross-subject consistency (Sub-C).

4.2.1 Ablation Study

Our ablation studies validate the necessity and contribution of performance-aware contrastive learning and transfer paradigms. Ablation results in Table 3 show that removing contrastive learning causes an 86% drop in temporal correlation performance, dropping T-Corr from 0.893 to 0.123, and R-Corr from 0.539 to near-zero (0.001). Adaptive transfer significantly improves performance correlations and clustering consistency compared to other transfer paradigms or no transfer. Moreover, adding θ improves timing and path-accuracy correlations and substantially reduces endpoint error ($0.072 \rightarrow 0.019$ with θ and 0.015 with θ+rotation angle), but rMSE goes down. Such as, θ components increase T-Corr +0.087 and R-Corr +0.121; S-Corr remains strong (> 0.90). These results indicate that adding target direction as an auxiliary input, along with normalized trajectory, restores asymmetry-related cues and improves performance.

4.2.2 Baseline Comparison

Existing trajectory analysis methods lack downstream applicability for motor control and rehabilitation practices Hu et al. (2023); Chen et al. (2024). We selected four methods for comparison

that closely matched study objectives: (1) STTraj2Vec Zhu et al. (2024), (2) Variational Auto-Encoders (VAEs) Ivanovic et al. (2020), (3) Sequence-to-Sequence Auto-Encoders (Seq2Seq) Sarkar & Ghose (2018); Wang et al. (2022), and (4) Trajectory Masked Autoencoders (Taj-MAE) Chen et al. (2023). We found that SMT-Learner outperformed with the best rMSE, Ep-Err, Curve-Err, and S-Corr, in both tests with D_1 (training and finetuned) and D_2 held-out evaluation (Table 4). However, STTraj2Vec optimized temporal/spatial continuity without incorporating outcome constraints (success/failure), yielding extremely high T-/R-Corr (L_2 norm of embedding grows with time or deviation). In motor tasks, failures or inefficient trials are longer and more deviant. If embedding magnitude amplifies only temporal/spatial characteristics, the same feature that boosts T-/R-Corr inversely relates to success, yielding negative S-Corr. SMT-Learner balanced temporal/spatial fidelity with performance-relevant structure. As a result, it maintains very high positive S-Corr while keeping competitive T-/R-Corr. Baseline comparison with Traj-MAE reflected that the similar studies (i.e., Forecast-mae Cheng et al. (2023), SEPT Lan et al. (2023)) would also fail to perform better in the investigated metrics as they lack performance-aware representation.

Table 4: Baseline comparison results

Method	rMSE	Ep-Err	Curve-Err	T-Corr	R-Corr	S-Corr
STTraj2Vec	0.386	0.095	3.666	**0.982**	**0.647**	-0.797
VAE	0.412	0.089	4.758	0.136	0.096	-0.135
Seq2Seq [48,49]	0.190	0.215	3.619	-0.996	-0.653	0.819
Traj-MAE	0.111	0.290	28.304	-0.960	-0.638	0.779
SMT-Learner$_{D_2}$	0.089	0.0944	1.867	0.735	0.522	0.9358
SMT-Learner$_{D_1}$	**0.086**	**0.072**	**1.577**	0.893	0.539	**0.970**

5 Limitations & Future Direction

SMT-Learner, while effective in capturing spatiotemporal dynamics of trajectory, has several constraints, including datasets, dimensionality, and generalizability. Embedding dimension, similarity thresholds, and sequential window sizes require systematic investigation for different movement trajectories across species, clinical conditions, and learning tasks. Moreover, the behavioral experiments were conducted in 2D space, which can be extended to 3D trajectories with minimal modification. We can simply modify input layer from $\mathcal{T}$ = {(x, y, t) | spatial coordinates + time} to $\mathcal{T}$ = {(x, y, z, t) | 3D coordinates + time} and normalizing 3D vector operations for position, rotation, and scaling. E-E analysis depends on embedded spaces and temporal continuity, and may be less sensitive when a learner suddenly shifts strategy, leading to discontinuous skill acquisition Newell (2014). Another limitation is that the findings on the unimanual vs bimanual visuomotor tasks represent a subset of motor skills, as the scope of this study only focused on repetitive motor tasks to understand learning behavior and micro-adaptation. However, other domains, such as gross motor skills, manual dexterity, or force production tasks, may require SMT-Learner fine-tuning using cross-task/cross-subject transfer to analyze E-E dynamics, which will be explored in the future.

6 Conclusions

Existing approaches to analyzing SMT data typically reduce complex motor trajectories to singular spatiotemporal parameters, such as movement accuracy or velocity. While important, this approach loses information about the dynamic nature of the action. Instade SMT-Learner, combined with an exploration-exploitation (E-E) metric to quantify fundamental aspects of motor skill learning across developmental contexts. Our computational & analytical approach bridges AI into neuromotor control, developmental psychology, and neurorehabilitation insights that could inform therapeutic and intervention planning by identifying learning strategy deficits to guide optimal therapy for populations with developmental disorders. Extensive experiments with two real datasets and hypothesis cross-validation revealed fundamental characteristics of skill acquisition, shifting from exploration-dominant to exploitation-dominant strategies over practice. In the future, adaptive transfer learning with data from different motor learning tasks and conditions would improve the capability for personalized therapy and modulate E-E balancing for individual learning profiles.

Ethics Statement

Human Subjects Protection. This study involves human subject data. We collected data of term and preterm-born children (D_1) to investigate motor skills learning and control strategies based on the IRB-approved experimental protocol. The parents or guardians of the child (as participants aged 5-8 years old) signed an informed consent form to share non-identifiable data for research purposes. We ensured HIPAA-compliant data storage and removed all identifiable information (e.g., name, date of birth, phone number) from the dataset. We used anonymous identifiers (e.g., MRTLRN###) only.

Reproducibility Statement

We supply all requisite materials and documentation to assure the reproducibility of the SMT-Learner framework. The source code implementation of the SMT-Learner architecture, encompassing the adaptive loss weighting mechanism, cross-task and cross-subject transfer learning modules, together with all experimental configurations, is accessible via an anonymous 4open.science repository Anonymous (2025). Furthermore, we have included a supplementary zip file comprising: (1) the complete codebase with README guidelines for environment configuration, data preprocessing, model training, and evaluation methodologies; (2) evaluation scripts that replicate all documented results; and (3) generated results, figures, and graphs.

References

Elysia Adams, Vann Chau, Kenneth J Poskitt, Ruth E Grunau, Anne Synnes, and Steven P Miller. Tractography-based quantitation of corticospinal tract development in premature newborns. *The Journal of pediatrics*, 156(6):882–888, 2010.

Alexandre Alahi, Kratarth Goel, Vignesh Ramanathan, Alexandre Robicquet, Li Fei-Fei, and Silvio Savarese. Social lstm: Human trajectory prediction in crowded spaces. In *Proceedings of the IEEE conference on computer vision and pattern recognition*, pp. 961–971, 2016.

John Allotey, Javier Zamora, Fiona Cheong-See, Madhavi Kalidindi, David Arroyo-Manzano, Elizabeth Asztalos, Joris AM van der Post, BW Mol, Derek Moore, Deidre Birtles, et al. Cognitive, motor, behavioural and academic performances of children born preterm: a meta-analysis and systematic review involving 64 061 children. *BJOG: An International Journal of Obstetrics & Gynaecology*, 125(1):16–25, 2018.

Anonymous. Smt-learner:movement trajectory learning to decode motor control strategies. `https://anonymous.4open.science/r/SMT-Learner-0D32/README.md`, 2025. Anonymous repository for review.

Nitin Nikamanth Appiah Balaji, Cynthia L Beaulieu, Jennifer Bogner, and Xia Ning. Traumatic brain injury rehabilitation outcome prediction using machine learning methods. *Archives of Rehabilitation Research and Clinical Translation*, 5(4):100295, 2023.

Nathaniel J Blanco and Vladimir M Sloutsky. Exploration, exploitation, and development: Developmental shifts in decision-making. *Child Development*, 95(4):1287–1298, 2024.

Judith Butepage, Michael J Black, Danica Kragic, and Hedvig Kjellstrom. Deep representation learning for human motion prediction and classification. In *Proceedings of the IEEE conference on computer vision and pattern recognition*, pp. 6158–6166, 2017.

Matthew S Cain, Edward Vul, Kait Clark, and Stephen R Mitroff. A bayesian optimal foraging model of human visual search. *Psychological science*, 23(9):1047–1054, 2012.

Silvia Campagnini, Chiara Arienti, Michele Patrini, Piergiuseppe Liuzzi, Andrea Mannini, and Maria Chiara Carrozza. Machine learning methods for functional recovery prediction and prognosis in post-stroke rehabilitation: a systematic review. *Journal of NeuroEngineering and Rehabilitation*, 19(1):54, 2022.

Bin Cao, Sinno Jialin Pan, Yu Zhang, Dit-Yan Yeung, and Qiang Yang. Adaptive transfer learning. In *proceedings of the AAAI Conference on Artificial Intelligence*, volume 24, pp. 407–412, 2010.

Frances A Carter and Michael E Msall. Long term functioning and participation across the life course for preterm nicu graduates. *Clinics in perinatology*, 45(3):501, 2018.

Hao Chen, Jiaze Wang, Kun Shao, Furui Liu, Jianye Hao, Chenyong Guan, Guangyong Chen, and Pheng-Ann Heng. Traj-mae: Masked autoencoders for trajectory prediction. In *Proceedings of the IEEE/CVF International Conference on Computer Vision*, pp. 8351–8362, 2023.

Ting Chen, Simon Kornblith, Mohammad Norouzi, and Geoffrey Hinton. A simple framework for contrastive learning of visual representations. In *International conference on machine learning*, pp. 1597–1607. PmLR, 2020.

Wei Chen, Yuxuan Liang, Yuanshao Zhu, Yanchuan Chang, Kang Luo, Haomin Wen, Lei Li, Yanwei Yu, Qingsong Wen, Chao Chen, et al. Deep learning for trajectory data management and mining: A survey and beyond. *arXiv preprint arXiv:2403.14151*, 2024.

Jie Cheng, Xiaodong Mei, and Ming Liu. Forecast-mae: Self-supervised pre-training for motion forecasting with masked autoencoders. In *Proceedings of the IEEE/CVF International Conference on Computer Vision*, pp. 8679–8689, 2023.

Yoo Jin Choo and Min Cheol Chang. Use of machine learning in stroke rehabilitation: a narrative review. *Brain & Neurorehabilitation*, 15(3):e26, 2022.

Mark M Churchland, Afsheen Afshar, and Krishna V Shenoy. A central source of movement variability. *Neuron*, 52(6):1085–1096, 2006.

RWI Cooke and L Foulder-Hughes. Growth impairment in the very preterm and cognitive and motor performance at 7 years. *Archives of disease in childhood*, 88(6):482–487, 2003.

Ashesh K Dhawale, Maurice A Smith, and Bence P Ölveczky. The role of variability in motor learning. *Annual review of neuroscience*, 40(1):479–498, 2017.

Kenji Doya. Complementary roles of basal ganglia and cerebellum in learning and motor control. *Current opinion in neurobiology*, 10(6):732–739, 2000.

Stacey C Dusing and Regina T Harbourne. Variability in postural control during infancy: implications for development, assessment, and intervention. *Physical therapy*, 90(12):1838–1849, 2010.

Fabrizio Ferrari, Claudio Gallo, Marisa Pugliese, Isotta Guidotti, Sara Gavioli, Elena Coccolini, Paola Zagni, Elisa Della Casa, Cecilia Rossi, Licia Lugli, et al. Preterm birth and developmental problems in the preschool age. part i: minor motor problems. *The journal of maternal-fetal & neonatal medicine*, 25(11):2154–2159, 2012.

Chelsea Finn, Xin Yu Tan, Yan Duan, Trevor Darrell, Sergey Levine, and Pieter Abbeel. Deep spatial autoencoders for visuomotor learning. In *2016 IEEE International Conference on Robotics and Automation (ICRA)*, pp. 512–519. IEEE, 2016.

LA Foulder-Hughes and RWI Cooke. Motor, cognitive, and behavioural disorders in children born very preterm. *Developmental medicine and child neurology*, 45(2):97–103, 2003.

Juan A Gallego, Matthew G Perich, Stephanie N Naufel, Christian Ethier, Sara A Solla, and Lee E Miller. Cortical population activity within a preserved neural manifold underlies multiple motor behaviors. *Nature communications*, 9(1):4233, 2018.

Tianyu Guo, Hong Liu, Zhan Chen, Mengyuan Liu, Tao Wang, and Runwei Ding. Contrastive learning from extremely augmented skeleton sequences for self-supervised action recognition. In *Proceedings of the AAAI conference on artificial intelligence*, volume 36, pp. 762–770, 2022.

Mijna Hadders-Algra. Variation and variability: key words in human motor development. *Physical therapy*, 90(12):1823–1837, 2010.

Kaiming He, Haoqi Fan, Yuxin Wu, Saining Xie, and Ross Girshick. Momentum contrast for unsupervised visual representation learning. In *Proceedings of the IEEE/CVF conference on computer vision and pattern recognition*, pp. 9729–9738, 2020.

Soheil Hor, Shubo Yang, Jaeho Choi, and Amin Arbabian. Mvdoppler: unleashing the power of multi-view doppler for micromotion-based gait classification. *Advances in Neural Information Processing Systems*, 36:58064–58074, 2023.

Danlei Hu, Lu Chen, Hanxi Fang, Ziquan Fang, Tianyi Li, and Yunjun Gao. Spatio-temporal trajectory similarity measures: A comprehensive survey and quantitative study. *IEEE Transactions on Knowledge and Data Engineering*, 36(5):2191–2212, 2023.

Boris Ivanovic, Karen Leung, Edward Schmerling, and Marco Pavone. Multimodal deep generative models for trajectory prediction: A conditional variational autoencoder approach. *IEEE Robotics and Automation Letters*, 6(2):295–302, 2020.

Mahdi M Kalayeh, Stephen Mussmann, Alla Petrakova, Niels da Vitoria Lobo, and Mubarak Shah. Understanding trajectory behavior: A motion pattern approach. *arXiv preprint arXiv:1501.00614*, 2015.

Alex Kendall, Yarin Gal, and Roberto Cipolla. Multi-task learning using uncertainty to weigh losses for scene geometry and semantics. In *Proceedings of the IEEE conference on computer vision and pattern recognition*, pp. 7482–7491, 2018.

TOMOKO Kitago and John W Krakauer. Motor learning principles for neurorehabilitation. *Handbook of clinical neurology*, 110:93–103, 2013.

Satoshi Kojima, Mimi H Kao, Allison J Doupe, and Michael S Brainard. The avian basal ganglia are a source of rapid behavioral variation that enables vocal motor exploration. *Journal of Neuroscience*, 38(45):9635–9647, 2018.

Sampo Kuutti, Richard Bowden, Yaochu Jin, Phil Barber, and Saber Fallah. A survey of deep learning applications to autonomous vehicle control. *IEEE Transactions on Intelligent Transportation Systems*, 22(2):712–733, 2020.

Zhiqian Lan, Yuxuan Jiang, Yao Mu, Chen Chen, and Shengbo Eben Li. Sept: Towards efficient scene representation learning for motion prediction. *arXiv preprint arXiv:2309.15289*, 2023.

Mindy F Levin, Heidi Sveistrup, and S Subramanian. Feedback and virtual environments for motor learning and rehabilitation. *Schedae*, 1:19–36, 2010.

Yan Liu, Danielle Balériaux, Martin Kavec, Thierry Metens, Julie Absil, Vincent Denolin, Anne Pardou, Freddy Avni, Patrick Van Bogaert, and Alec Aeby. Structural asymmetries in motor and language networks in a population of healthy preterm neonates at term equivalent age: a diffusion tensor imaging and probabilistic tractography study. *Neuroimage*, 51(2):783–788, 2010.

Jed A Long and Trisalyn A Nelson. A review of quantitative methods for movement data. *International Journal of Geographical Information Science*, 27(2):292–318, 2013.

Mingsheng Long, Yue Cao, Jianmin Wang, and Michael Jordan. Learning transferable features with deep adaptation networks. In *International conference on machine learning*, pp. 97–105. PMLR, 2015.

Ilya Loshchilov and Frank Hutter. Decoupled weight decay regularization. *arXiv preprint arXiv:1711.05101*, 2017.

Yael Mandelblat-Cerf, Rony Paz, and Eilon Vaadia. Trial-to-trial variability of single cells in motor cortices is dynamically modified during visuomotor adaptation. *Journal of Neuroscience*, 29(48): 15053–15062, 2009.

Ana I Maqueda, Antonio Loquercio, Guillermo Gallego, Narciso García, and Davide Scaramuzza. Event-based vision meets deep learning on steering prediction for self-driving cars. In *Proceedings of the IEEE conference on computer vision and pattern recognition*, pp. 5419–5427, 2018.

Matteo Menolotto, Dimitrios-Sokratis Komaris, Salvatore Tedesco, Brendan O'Flynn, and Michael Walsh. Motion capture technology in industrial applications: A systematic review. *Sensors*, 20 (19):5687, 2020.

Md Raihan Mia, Sheikh Iqbal Ahamed, Alissa Fial, and Samuel Nemanich. A scoping review on mobile health technology for assessment and intervention of upper limb motor function in children with motor impairments. *Games for Health Journal*, 13(3):135–148, 2024.

M Berk Mirza, Rick A Adams, Christoph Mathys, and Karl J Friston. Human visual exploration reduces uncertainty about the sensed world. *PloS one*, 13(1):e0190429, 2018.

Sergio L Molina, Tim S Bott, and David F Stodden. Applications of the speed–accuracy trade-off and impulse-variability theory for teaching ballistic motor skills. *Journal of Motor Behavior*, 2019.

Dave G Mumby, Stephane Gaskin, Melissa J Glenn, Tania E Schramek, and Hugo Lehmann. Hippocampal damage and exploratory preferences in rats: memory for objects, places, and contexts. *Learning & memory*, 9(2):49–57, 2002.

Margit Alt Murphy, Carin Willén, and Katharina S Sunnerhagen. Kinematic variables quantifying upper-extremity performance after stroke during reaching and drinking from a glass. *Neurorehabilitation and neural repair*, 25(1):71–80, 2011.

Karl M Newell. Change in movement and skill: Learning, retention, and transfer. In *Dexterity and its development*, pp. 393–429. Psychology Press, 2014.

Bence P Ölveczky, Aaron S Andalman, and Michale S Fee. Vocal experimentation in the juvenile songbird requires a basal ganglia circuit. *PLoS biology*, 3(5):e153, 2005.

Cynthia Ortinau and Jeffrey Neil. The neuroanatomy of prematurity: normal brain development and the impact of preterm birth. *Clinical Anatomy*, 28(2):168–183, 2015.

Sarah Palmis, Jeremy Danna, Jean-Luc Velay, and Marieke Longcamp. Motor control of handwriting in the developing brain: A review. *Developmental Dysgraphia*, pp. 123–140, 2019.

Ravi Mangal Patel. Short-and long-term outcomes for extremely preterm infants. *American journal of perinatology*, 33(03):318–328, 2016.

Réjean Plamondon and Adel M Alimi. Speed/accuracy trade-offs in target-directed movements. *Behavioral and brain sciences*, 20(2):279–303, 1997.

Chandra Prakash, Rajesh Kumar, and Namita Mittal. Recent developments in human gait research: parameters, approaches, applications, machine learning techniques, datasets and challenges. *Artificial Intelligence Review*, 49:1–40, 2018.

Sara Rapuc, Blaž Stres, Ivan Verdenik, Miha Lučovnik, and Damjan Osredkar. Uncovering early predictors of cerebral palsy through the application of machine learning: a case–control study. *BMJ Paediatrics Open*, 8(1):e002800, 2024.

David J Reinkensmeyer, Etienne Burdet, Maura Casadio, John W Krakauer, Gert Kwakkel, Catherine E Lang, Stephan P Swinnen, Nick S Ward, and Nicolas Schweighofer. Computational neurorehabilitation: modeling plasticity and learning to predict recovery. *Journal of neuroengineering and rehabilitation*, 13:1–25, 2016.

Chiara Renso, Miriam Baglioni, Jose Antonio F de Macedo, Roberto Trasarti, and Monica Wachowicz. How you move reveals who you are: understanding human behavior by analyzing trajectory data. *Knowledge and information systems*, 37:331–362, 2013.

Andrey Rudenko, Luigi Palmieri, Michael Herman, Kris M Kitani, Dariu M Gavrila, and Kai O Arras. Human motion trajectory prediction: A survey. *The International Journal of Robotics Research*, 39(8):895–935, 2020.

Fernando J Santos, Rodrigo F Oliveira, Xin Jin, and Rui M Costa. Corticostriatal dynamics encode the refinement of specific behavioral variability during skill learning. *Elife*, 4:e09423, 2015.

Meenakshi Sarkar and Debasish Ghose. Sequential learning of movement prediction in dynamic environments using lstm autoencoder. *arXiv preprint arXiv:1810.05394*, 2018.

Matteo Saveriano, Fares J Abu-Dakka, Aljaž Kramberger, and Luka Peternel. Dynamic movement primitives in robotics: A tutorial survey. *The International Journal of Robotics Research*, 42(13): 1133–1184, 2023.

Cyril Schneider, Line Nadeau, Chantal Bard, Julie Lambert, Annette Majnemer, Francine Malouin, Philippe Robaey, Pascale St-Amand, and Rejean Tessier. Visuo-motor coordination in 8-year-old children born pre-term before and after 28 weeks of gestation. *Developmental neurorehabilitation*, 11(3):215–224, 2008.

Wilko Schwarting, Javier Alonso-Mora, and Daniela Rus. Planning and decision-making for autonomous vehicles. *Annual Review of Control, Robotics, and Autonomous Systems*, 1(1):187–210, 2018.

Stephen H Scott and John F Kalaska. Reaching movements with similar hand paths but different arm orientations. i. activity of individual cells in motor cortex. *Journal of neurophysiology*, 77(2): 826–852, 1997.

Stephen H Scott, Paul L Gribble, Kirsten M Graham, and D William Cabel. Dissociation between hand motion and population vectors from neural activity in motor cortex. *Nature*, 413(6852): 161–165, 2001.

Ketul Shah, Anshul Shah, Chun Pong Lau, Celso M de Melo, and Rama Chellappa. Multi-view action recognition using contrastive learning. In *Proceedings of the ieee/cvf winter conference on applications of computer vision*, pp. 3381–3391, 2023.

Peter Shaw, Jakob Uszkoreit, and Ashish Vaswani. Self-attention with relative position representations. *arXiv preprint arXiv:1803.02155*, 2018.

Xiaodan Shi, Haoran Zhang, Wei Yuan, and Ryosuke Shibasaki. Metatraj: meta-learning for cross-scene cross-object trajectory prediction. *IEEE Transactions on Intelligent Transportation Systems*, 24(12):14000–14009, 2023.

Joshua S Shimony, Christopher D Smyser, Graham Wideman, Dimitrios Alexopoulos, Jason Hill, John Harwell, Donna Dierker, David C Van Essen, Terrie E Inder, and Jeffrey J Neil. Comparison of cortical folding measures for evaluation of developing human brain. *Neuroimage*, 125:780–790, 2016.

Lior Shmuelof, John W Krakauer, and Pietro Mazzoni. How is a motor skill learned? change and invariance at the levels of task success and trajectory control. *Journal of neurophysiology*, 108(2): 578–594, 2012.

Bouwien Smits-Engelsman, Emmanuel Bonney, and Gillian Ferguson. Motor skill learning in children with and without developmental coordination disorder. *Human Movement Science*, 74: 102687, 2020.

N Smyrnis, I Evdokimidis, TS Constantinidis, and G Kastrinakis. Speed-accuracy trade-off in the performance of pointing movements in different directions in two-dimensional space. *Experimental Brain Research*, 134:21–31, 2000.

Sijie Song, Cuiling Lan, Junliang Xing, Wenjun Zeng, and Jiaying Liu. An end-to-end spatio-temporal attention model for human action recognition from skeleton data. In *Proceedings of the AAAI conference on artificial intelligence*, volume 31, 2017.

Laure Spieser, Mathieu Servant, Thierry Hasbroucq, and Borís Burle. Beyond decision! motor contribution to speed–accuracy trade-off in decision-making. *Psychonomic Bulletin & Review*, 24 (3):950–956, 2017.

Alicia J Spittle, Jennifer L McGinley, Deanne Thompson, Ross Clark, Tara L FitzGerald, Benjamin F Mentiplay, Katherine J Lee, Joy E Olsen, Alice Burnett, Karli Treyvaud, et al. Motor trajectories from birth to 5 years of children born at less than 30 weeks' gestation: early predictors and functional implications. protocol for a prospective cohort study. *Journal of physiotherapy*, 62(4): 222–223, 2016.

Karel Svoboda and Nuo Li. Neural mechanisms of movement planning: motor cortex and beyond. *Current opinion in neurobiology*, 49:33–41, 2018.

Kurt A Thoroughman and Reza Shadmehr. Learning of action through adaptive combination of motor primitives. *Nature*, 407(6805):742–747, 2000.

Maria José Uparela-Reyes, Lina María Villegas-Trujillo, Jorge Cespedes, Miguel Velásquez-Vera, and Andrés M Rubiano. Usefulness of artificial intelligence in traumatic brain injury: A bibliometric analysis and minireview. *World Neurosurgery*, 2024.

Karoliina Uusitalo, Leena Haataja, Anna Nyman, Liisi Ripatti, Mira Huhtala, Päivi Rautava, Liisa Lehtonen, Riitta Parkkola, Katri Lahti, Mari Koivisto, et al. Preterm children's developmental coordination disorder, cognition and quality of life: a prospective cohort study. *BMJ Paediatrics Open*, 4(1):e000633, 2020.

Carolien J van Andel, Nienke Wolterbeek, Caroline AM Doorenbosch, DirkJan HEJ Veeger, and Jaap Harlaar. Complete 3d kinematics of upper extremity functional tasks. *Gait & posture*, 27(1): 120–127, 2008.

Ashish Vaswani, Noam Shazeer, Niki Parmar, Jakob Uszkoreit, Llion Jones, Aidan N Gomez, Łukasz Kaiser, and Illia Polosukhin. Attention is all you need. *Advances in neural information processing systems*, 30, 2017.

Paolo Viviani and Carlo Terzuolo. Trajectory determines movement dynamics. *Neuroscience*, 7(2): 431–437, 1982.

Mai-Anh T Vu, Tülay Adalı, Demba Ba, György Buzsáki, David Carlson, Katherine Heller, Conor Liston, Cynthia Rudin, Vikaas S Sohal, Alik S Widge, et al. A shared vision for machine learning in neuroscience. *Journal of Neuroscience*, 38(7):1601–1607, 2018.

Chao Wang, Fangzheng Lyu, Sensen Wu, Yuanyuan Wang, Liuchang Xu, Feng Zhang, Shaowen Wang, Yongheng Wang, and Zhenhong Du. A deep trajectory clustering method based on sequence-to-sequence autoencoder model. *Transactions in GIS*, 26(4):1801–1820, 2022.

Tongzhou Wang and Phillip Isola. Understanding contrastive representation learning through alignment and uniformity on the hypersphere. In *International conference on machine learning*, pp. 9929–9939. PMLR, 2020.

Dirk U Wulff, Jonas MB Haslbeck, Pascal J Kieslich, Felix Henninger, and Michael Schulte-Mecklenbeck. Mouse-tracking: Detecting types in movement trajectories. In *A handbook of process tracing methods*, pp. 131–145. Routledge, 2019.

Lindsay E Wyatt, Patrick A Hewan, Jeremy Hogeveen, R Nathan Spreng, and Gary R Turner. Exploration versus exploitation decisions in the human brain: A systematic review of functional neuroimaging and neuropsychological studies. *Neuropsychologia*, 192:108740, 2024.

Lei Zhang and Xinbo Gao. Transfer adaptation learning: A decade survey. *IEEE Transactions on Neural Networks and Learning Systems*, 35(1):23–44, 2022.

Huiyu Zhou and Huosheng Hu. Human motion tracking for rehabilitation—a survey. *Biomedical signal processing and control*, 3(1):1–18, 2008.

Jiahui Zhu, Xinzheng Niu, Fan Li, Yixuan Wang, Philippe Fournier-Viger, and Kun She. Sttraj2vec: A spatio-temporal trajectory representation learning approach. *Knowledge-Based Systems*, 300: 112207, 2024.

A Appendix

A.1 Datasets

A.1.1 D_1: Human Movement Data.

D_1 contains 16320 trajectories of term (73.5%) and preterm (26.5%) born children. Data was collected using an iPad-based visuomotor game, designed for unimanual and bimanual motor learning using controlled psychophysical tasks. We conducted a cross-sectional multi-visitation observation study to assess motor skills learning and performance in term and preterm children aged 5-8 years. This study aimed to measure a child's development and overall abilities to learn new motor tasks and establish causal links between motor learning and performance. We explored the relationship between motor planning and execution networks for completing functional tasks and identified primary contributors to overall motor development. The university's Institutional Review Board (IRB) approved study protocol.

Study Protocol: We examined unimanual and bimanual motor learning using controlled psychophysical tasks. We created a straightforward yet challenging visuomotor task that tested how participants learned a new mapping between joystick and cursor movement. The experimental tasks (Figure 5) involve moving a cursor on an iPad 12.9-inch screen (cartoon bee) to a visual target (flower) using a joystick. The mapping of joystick direction to cursor movement systematically varied. For the unimanual task, a single two-dimensional joystick was used with the direction map inverted (e.g., moving the joystick upward moves the cursor downward, and moving the joystick rightward moves the cursor leftward). For the bimanual task, two one-dimensional (vertical movement only) joysticks were controlled with each hand, with the left joystick controlling the cursor vertically and the right joystick controlling the cursor horizontally. The unimanual learning task was a mirror reversal task. Furthermore, the bimanual task involved the non-intuitive 90° rotation of the directionality of one joystick, which was even more challenging. These adaptations, while easy for adults to learn, were challenging for young children. Thus, we propose that the tasks were appropriately complex for the age (5-8 years old) of the participants performing them.

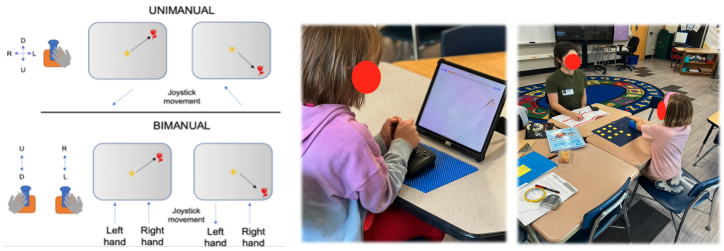

(a) (b)

Figure 5: Study protocols and data collection (a) Experimental design of the tasks in an iPad game (unimanual and bimanual tasks, and (b) A session of participants' data collection using the mHealth system in an elementary school networks

Task Parameters: For each trial, the cursor starts in the center of the screen. Six targets within each of the four quadrants of the 2D screen were selected randomly; thus, the participant moved to 24 targets during each practice block. The variability in the initial location of the target should enhance motor learning based on the effects of a variable practice schedule. The participant has 10 seconds to complete the trial and reach the target. A new trial begins if the cursor does not reach the target in under 10 seconds. Visual feedback on trial success (smiley face) or failure ("Try again" message) was provided. To prevent participants from moving in a unidirectional manner during the bimanual task (i.e., moving only the left joystick to move vertically, then the

Table 5: Participant characteristics

Characteristics	**Term**	**Preterm**
# of Participant (N)	50	18
Age Group (N, %) 5-6 7-8	19 (38.0%) 31 (62.0%)	7 (38.8%) 11 (61.1%)
Gestational Age (weeks), mean ± SD	39 ± 2	31 ± 3
MABC-2 percentile, mean ± 95%CI	39.91±0.75	23.61±0.87

right joystick to move horizontally), cursor movement was programmed to advance only when both joysticks are moved. In each trial, we recorded source and target destinations, (x,y) coordinates as continuous movement paths with time dimension at 120 Hz sampling rate.

Participants & Data Collection: We collected data from 72 participants, 68 of whom completed all blocks of tasks successfully on Day-1, Day-2, and Day-7. Table 5 shows a summary of the participants' characteristics. Along with the game data, we tested participants' standard battery assessment (MABC-2: Movement Assessment Battery for Children). Among term and preterm children, we found a significant difference in MABC-2 percentiles (23.61±0.87 vs. 39.91±0.75, p<0.001), demonstrating substantial clinical and neurodevelopmental validation. Each of the participants practiced 6 blocks of 24 trials each, completed on Day 1, with 1-2 minutes of rest between each block. To examine retention, a single block of 24 trials was repeated on Days 2 and 7 (retention blocks). A total of 680 blocks/sessions of data was collected with 680x24 trials. This dataset contains 16320 trajectories of term (73.5%) and preterm (26.5%) children, where each task contains 50% the trajectories.

A.1.2 D_2: Non-human Reaching Movement

D_2 contains non-human primates' arm reaching trajectories Scott et al. (2001); Scott & Kalaska (1997), a groundbreaking study investigated the neural basis of motor control and hand movement kinematics. Three rhesus monkeys were highly trained to perform horizontal planar reaching movements wearing mechanical exoskeletons. The task was centered on reaching a target arranged in a circle with five experimental conditions (e) and collected spatiotemporal positions, velocity, and joint angles with neural recordings. Each hand trajectory contains (x, y, t) coordinates, matching the expected input format for SMT-Learner. An example of experiment reaching trajectories to uniformly distributed targets at 0, 45, 90, 135, 180, 225, 270, and 315 degrees are illustrated in Figure 6. This dataset includes 16 unique reaching directions with standardized durations (∼576ms). We used a total of 23639 trajectories from a total of 587 sessions, where 75% of the sessions contained 48 trials in four experimental tasks.

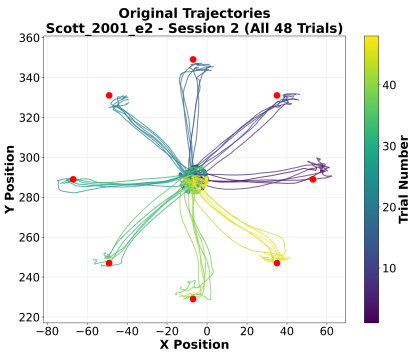

Figure 6: Examples of monkey's hand movement trajectories of e2 experiment

A.2 Experimental Setup

Experiments were conducted using NVIDIA GH200 Superchips (H100 configured with 80 GB SXM5, 26 vCPUS, 225 GiB RAM and 2.8 TiB SSD). We followed a two-phase training and evaluation approach with two datasets D_1 and D_2. In our first phase, SMT-Learner was pre-trained using D_1 with a 90:10 split ratio for the train and validation partitions, and 32 SMT as the input batch size. The total joint loss combines reconstruction and multi-contrastive objectives as $\mathcal{L}_{total} = \mathcal{L}_r + \mathcal{L}_m$. The model was trained for each component of contrastive loss separately, as well as multi-contrastive loss by combining a weighted function of loss components. With 50 epochs, early stopping was imposed based on validation loss, and the AdamW optimizer was used with a learning rate of 0.0001 Loshchilov & Hutter (2017). We evaluated four experimental conditions in pretraining/finetuning paradigms to separate the cross-task and cross-subject transfer effects on adaptive transfer, as follows.

1. Exp1: Pretrain on D_1 → test on D_1 → zero-shot on D_2 (held-out)
2. Exp2: Cross-Task transfer: Pretrain on D_1 Unimanual → Test on D_1 Bimanual → Zero-shot on D_2 (Experimental task 1: Scott_2001_e1)
3. Exp3: Cross-Subject transfer: Pretrain on D_1 (Cohort==Term) → test on D_1 (Cohort == Preterm) → Zero-shot on D_2
4. Exp4: Adaptive transfer: Combine Exp2 and Exp3 → test on D_1 → zero-shot on D_2

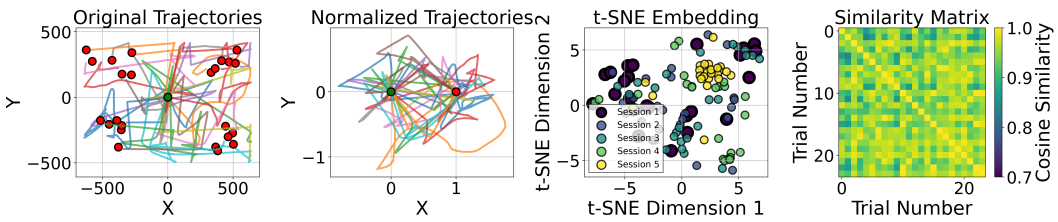

(a) Participant MTRLRN070 practice at day-1 [Unimanual Task]

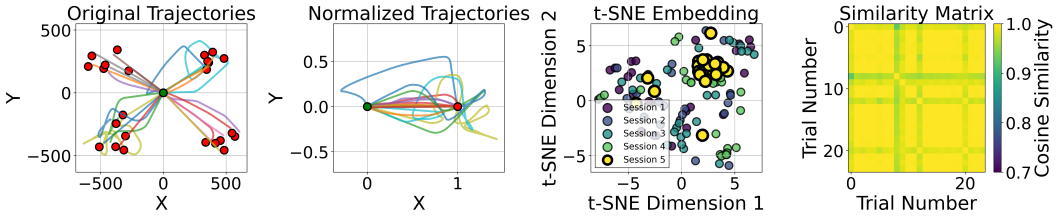

(b) Participant MTRLRN070 retention at day-7 [Unimanual Task]

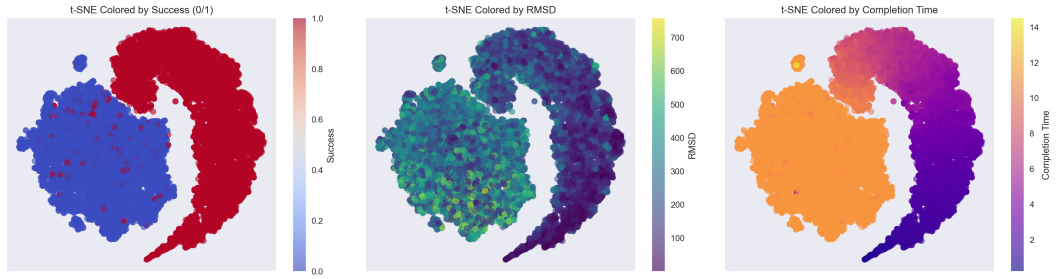

(c) 2D tSNE visualization of the embedded space colored by (left to right) Success, RMSD, and Completion time

Figure 7: Trajectory representations in embedding space. (a–b) Embedded layout and trial-by-trial trajectory similarity for a Unimanual participant. (c) t-SNE shows tighter clusters for higher-skill learners (moon shape); unsuccessful trials form a compact "ball" cluster and are associated with longer durations and greater path deviation.

A.3 Sensitivity and Clustering Analysis

Figures 7a and 7b compare a participant's embedded trial-by-trial trajectory similarity on the first practice day versus Day-7 retention. At Day 7, embeddings exhibit closer, more stable neighborhoods and reduced dispersion, indicating learning adaptivity and a shift toward exploitative control. The 2D t-SNE projection (Fig. 7c) separates the D_1 latent space by motor performance, where higher motor performance trials form close clusters near the task manifold, whereas lower-performing trials cluster in diffuse regions associated with longer competition time and larger path deviations (RMSD).

We conducted a sensitivity analysis on D_1 over window $W \in \{5, 10, 25, 50, 75, 100, 150, 225, 300, 450\}$, decay $\alpha \in \{0.05, 0.1, 0.2, 0.3, 0.5\}$, and $(\beta_1, \beta_2) \in \{0.1, 0.3, 0.5, 0.7, 0.9\}^2$ to identify stable parameters for the E–E metric calculation. Three convergent patterns founded in the chosen configuration:

i. S-/R-/T-Corr curves rise sharply and plateaued near $W \approx 120$ aligning with a participant's full trial count (Figure 8);

ii. Normalized E–E varies $< 6\%$ (CV) across $\alpha \in [0.05, 0.3]$, $\beta_1 \in [0.05, 0.2]$, $\beta_2 \in [0.3, 0.9]$. The setting $\alpha = 0.05$, $\beta_1 = 0.10$, $\beta_2 = 0.90$ balances strong early exploration ($\beta_2 \gg \beta_1$) with a smooth decay to a modest baseline (β_1);

iii. The MIN distance (minimum Euclidean distance in embedding to any prior trial within the decayed window) consistently outperformed KNN averaging on ranking quality, indicating sharper novelty discrimination (Table 6a).

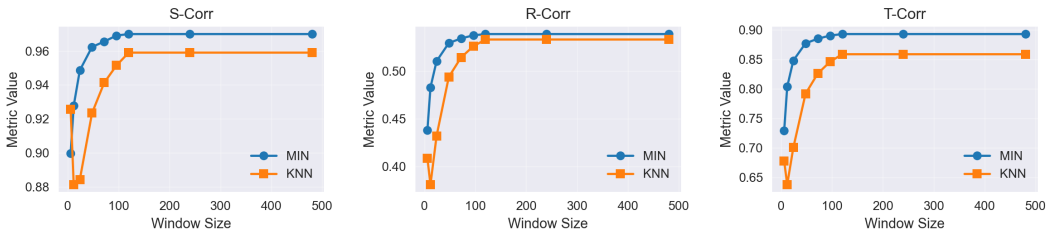

Figure 8: Sensitivity curves comparing MIN vs. KNN. Curves plateau near $W \approx 120$; MIN consistently dominates KNN across decay settings.

Table 6: Novelty metric comparison and clustering diagnostics on SMT-Learner embeddings.

(a) Novelty metric comparison

Metric variant	ROC AUC	PR AUC	F1
min_dist (MIN)	**0.5521**	**0.5403**	**0.6994**
knn_avg (KNN)	0.4962	0.5026	0.6927

PR: Precision–Recall; AUC: Area Under the Curve.
min_dist: minimum distance to any prior trial within window W
knn_avg: mean distance to the K nearest prior trials

(b) Clustering diagnostics

Algo	k/ε	Silhouette	Purity
KMeans	3	0.478900	0.962428
KMeans	5	0.405406	0.982313
KMeans	7	0.290197	0.971298
DBSCAN	0.5	0.361061	**1.000000**
DBSCAN	1.0	**0.670152**	0.999547
DBSCAN	1.5	0.253241	0.998204

Clustering diagnostics on SMT-Learner embeddings confirmed separability with density-based methods, results in Table 6b. DBSCAN at $\varepsilon = 1.0$ achieves the highest silhouette score with near-perfect purity, reinforcing that the latent geometry supports separable task–performance manifolds. These diagnostics substantiate the parameterization used for downstream E–E estimation.

A.4 Case Study: Optimal Strategy Detection

Our framework is capable to detect motor tasks with potentially multiple optimal strategies. We reasoned that the optimal solution to our experimental task was to move to the target in the most efficient path, thereby reducing uncertainty and physiological effort. Optimal solutions could also vary dependent on other environmental conditions (presence of reward, verbal instructions). To provide further clarification, we conducted a case study analysis showing two distinct optimal strategies: (1) Curvature optimization to near-straight paths (mostly used for unimanual), and (2) Stepwise optimal movement with directional changes (mostly used for bimanual). The Table 7 shows the case study results with participants MRTLRN070 and MRTLRN015 (Figure 9 illustrates original trajectories). The E-E framework successfully captured both strategies with a significant E-E ratio reduction (curvature: $0.56 \rightarrow 0.04$, and stepwise: $0.57 \rightarrow 0.07$). Curvature optimization resulted in highly consistent smooth movements (lower final E-E), while stepwise control maintained inherent variability in segmented movements (higher final E-E). This case study demonstrates that SMT-Learner can

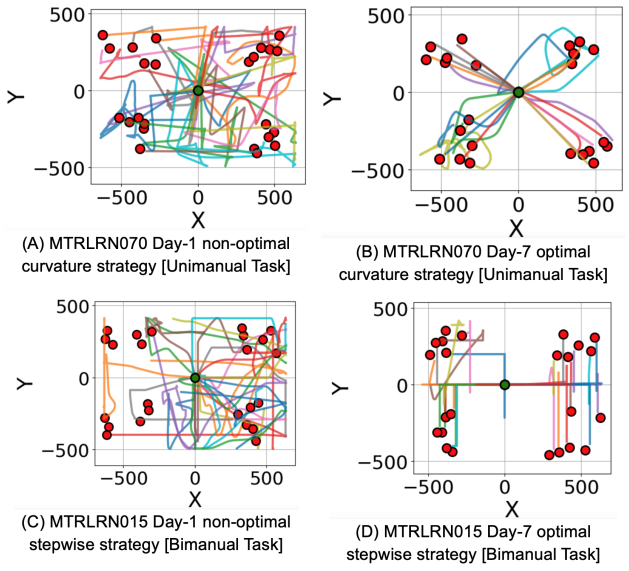

Figure 9: Case study: example of curvature and stepwise optimal movement strategies in motor skill learning

handle multiple optimal strategies in the movement space, enabling quantitative differentiation of strategic signatures.

Table 7: Case study results showing difference between two distinct optimal strategies (participant MTRLRN070: Curvature and MTRLRN015: Stepwise)

Strategy	E-E Ratio		Success Rate		Completion Time (s)		RMSD	
	Day-1	Day-7	Day-1	Day-7	Day-1	Day-7	Day-1	Day-7
Curvature	0.5579	**0.0433**	91.67%	**100%**	7.34	**2.36**	152.74	**35.84**
Stepwise	0.5718	0.0681	20.83%	**100%**	10.19	5.10	270.91	152.85

A.5 Capturing Motor Control Beyond Geometry: SMT-Learner Embeddings

We computed E–E ratios on normalized trajectories and in the learned embedding using $N = 1000$ random samples from D_1 Term and Preterm cohorts. As shown in Figure 10, embedding-space E–E yields stable, interpretable effects with tight confidence intervals (CIs), whereas trajectory-space E–E exhibits large-magnitude, high-variance estimates driven by residual geometric/scale variability despite normalization. For early→late learning, the embedding difference is 0.1503 with a narrow 95% CI $[0.1329, 0.1680]$, while the trajectory estimate is 162.71 with a very wide CI $[1.79, 441.73]$. For Preterm–Term (bimanual), the embedding difference is 0.0075 with CI $[-0.0229, 0.0337]$, whereas the trajectory-based mean difference is -274.75 with a wide CI $[-1169.24, 112.60]$. These results indicate that SMT-Learner's embeddings capture higher-order control structure beyond geometric variability and provide a scale-stable E–E metric.

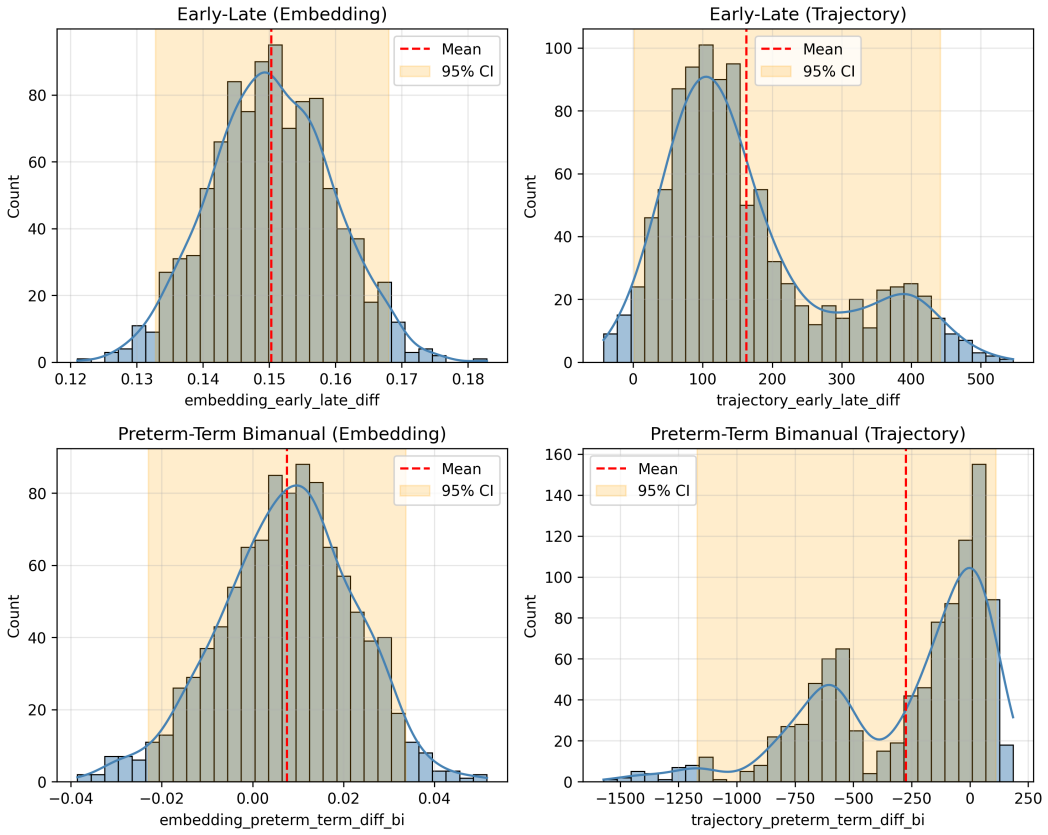

Figure 10: Randomized sampling distributions of E–E differences in embedding space vs. normalized trajectory space ($N = 1000$). Embedding E–E shows tight, stable CIs; trajectory E–E exhibits high variance due to residual geometric/scale effects.